

# Latent Iterative Refinement Flow: A Geometric-Constrained Approach for Few-Shot Generation

Songtao Li<sup>1,3</sup>, Zhenyu Liao<sup>2</sup>, Tianqi Hou<sup>4</sup> Ting Gao\*<sup>1,3</sup>

<sup>1</sup>School of Mathematics and Statistics, Huazhong University of Science and Technology, Wuhan 430074, China

<sup>2</sup>School of Electronic Information and Communications, Huazhong University of Science and Technology, Wuhan, China

<sup>3</sup>Center for Mathematical Science, Huazhong University of Science and Technology, Wuhan 430074, China <sup>4</sup> Huawei

songtao\_li@hust.edu.cn, zhenyu\_liao@hust.edu.cn, thou@connect.ust.hk, tgao0716@hust.edu.cn

## Abstract

Few-shot generation, the synthesis of high-quality and diverse samples from limited training data, remains a significant challenge in generative modeling. Existing methods trained from scratch often fail to overcome overfitting and mode collapse, and fine-tuning large models can inherit biases while neglecting the crucial geometric structure of the latent space. To address these limitations, we introduce **Latent Iterative Refinement Flow (LIRF)**, a novel approach that reframes few-shot generation as the progressive densification of geometrically structured manifold. LIRF establishes a stable latent space using an autoencoder trained with our novel **manifold-preservation loss**  $L_{\text{manifold}}$ . This loss ensures that the latent space maintains the geometric and semantic correspondence of the input data. Building on this, we propose an iterative generate-correct-augment cycle. Within this cycle, candidate samples are refined by a geometric **correction operator**, a provably contractive mapping that pulls samples toward the data manifold while preserving diversity. We also provide the **Convergence Theorem** demonstrating a predictable decrease in Hausdorff distance between generated and true data manifold. These findings are also supported by our experimental results: A detailed convergence analysis on MNIST demonstrates how our iterative approach consistently improves sample quality and manifold density. On the CIFAR-10 benchmark (10% data), LIRF achieved an FID of 30.29, significantly outperforming existing baselines. We also demonstrate the framework’s scalability by generating coherent, high-resolution images on AFHQ-Cat. Ablation studies confirm that both the manifold-preserving latent space and the contractive correction mechanism are critical components of this success. Ultimately, LIRF provides a solution for data-scarce generative modeling that is not only theoretically grounded but also highly effective in practice. We will make our code publicly available.

## Introduction

Generative model has achieved remarkable success in synthesizing high-fidelity data (Dinh, Sohl-Dickstein, and Bengio 2016; Karras et al. 2022), but this often depends on the vast quantity and diversity of available training data in general domains. In many specific application areas, gathering sufficiently large-scale datasets is challenging or even unfeasible due to constraints on imaging expense, subject type, image quality, privacy, or copyright status. This makes few-shot generation—the task of creating diverse and realis-

tic samples from only a handful of examples—a formidable challenge. In this low-data environment, conventional models are prone to severe overfitting, often devolving into memorizing the training set or suffering from mode collapse. This prevents them from capturing the true underlying data distribution. While recent approaches attempt to address this by fine-tuning large pre-trained models(Ruiz et al. 2023; Duan et al. 2024) or identifying sparse “lottery tickets” within GANs (Chen et al. 2021), they often inherit the biases and domain limitations of the foundational models. Crucially, many of these methods overlook a fundamental aspect of the problem: the geometric structure of the latent space, which is critical for meaningful generalization from sparse data. An unstructured latent space can distort the relationships between samples (Upchurch et al. 2017), making it exceedingly challenging to generate novel, coherent variations from a few anchor points.

To address these limitations, we reframe the few-shot generation problem. Instead of directly learning a complex distribution in the high-dimensional pixel space, we propose to first map the data onto a geometrically structured latent manifold and then progressively densify this manifold. We introduce **Latent Iterative Refinement Flow (LIRF)**, a novel and theoretically guaranteed framework that learns to generate high-fidelity samples by iteratively augmenting its training data. Our approach is founded on two synergistic principles. First, we establish a novel embedding approach by training an autoencoder with the manifold-preserving loss  $L_{\text{manifold}}$ . This objective ensures that the latent space preserves the local geometric structure of the original data.

On top of this structured latent space, LIRF implements a robust iterative loop: generation, correction, and augmentation. At each iteration, a flow-matching model (Lipman et al. 2023) first generates candidate samples. These candidate samples are then refined by a novel geometric **Correction Operator**, a map which is proved to be a contraction mapping, thereby guaranteeing that the refinement process is stable and robustly pulls candidate samples toward the anchor data manifold. This generate-correct-augment cycle progressively densifies the latent manifold, allowing the generative model to learn an increasingly accurate representation of the data distribution. The efficiency of this entire procedure is not solely demonstrated empirically, but also formally guaranteed with the **Convergence Theorem** that

our iterative process converges toward the true data distribution. Our primary contributions are:

1. We propose Latent Iterative Refinement Flow (LIRF), a novel flow matching training paradigm for few-shot generation. It progressively densifies the latent manifold through generate-correct-augment cycle.
2. We design a manifold-preserving loss  $L_{manifold}$  and provide theoretical guarantee for similar geometric structure in latent space, a key prerequisite for meaningful few-shot generation.
3. We introduce a geometrically principled correction mechanism and prove it is a contraction mapping, ensuring the stability and effectiveness of our iterative refinement loop.
4. We prove the convergence of LIRF framework, establishing that the Hausdorff distance between the generated manifold and the true data distribution decreases along iterations.

Through extensive experiments on MNIST, CIFAR-10, and high-resolution AFHQ-Cat datasets, we demonstrate that LIRF significantly outperforms other few-shot generation methods. Our ablation studies confirm that our manifold-preserving latent space and the contractive correction operator are essential for its success. Our work presents an accurate, reliable, and domain-agnostic way for generative modeling in low-data regimes.

## Related Work

**Flow Matching.** Flow-based generative models leverage normalizing flows to transform a simple base distribution into a complex target distribution through invertible mappings, enabling exact likelihood computation and efficient sampling like NICE(Dinh, Krueger, and Bengio 2014) and RealNVP(Dinh, Sohl-Dickstein, and Bengio 2016). Lipman et al. introduce Flow Matching as a simulation-free method that generalizes diffusion models and supports efficient probability paths, such as those based on Optimal Transport. Its compatibility with various probability paths, including linear displacement interpolation, enhances its flexibility for diverse generative tasks (Liu, Gong, and Liu 2022). A comprehensive review by Gat et al. (Lipman et al. 2024) provides further insights into Flow Matching’s foundations and applications. And then Dao et al. extend Flow Matching to the latent space of pretrained autoencoders, improving computational efficiency and scalability for high-resolution image synthesis like label-conditioned image generation and image inpainting, with results validated on datasets like CelebA-HQ and FFHQ(Dao et al. 2023).

**Generative Model on Limited Data.** Early attempts to synthesize new classes from scant data relied on meta-learning GANs. Most GAN-based methods fine-tune only a subset of weights or latent codes to avoid catastrophic overfitting. Chen et al. leverages the lottery ticket hypothesis to identify sparse GAN tickets that achieve superior performance than full GANs in the data-scarce scenarios(Chen et al. 2021), whereas WeditGAN adapts intermediate  $w$  codes with linear offsets learned from a handful

of examples(Duan et al. 2024). Diffusion model counterparts adopt a similar strategy: DreamBooth injects an identifier token and fine-tunes text-image diffusion models on 3–5 images(Ruiz et al. 2023), while Patch Diffusion train the diffusion model on many image patches to improve data efficiency (Wang et al. 2023). Beyond single-task tuning, Few-Shot Diffusion Models Escape the Curse of Dimensionality (Yang et al. 2024) provide the first sample-complexity analysis for diffusion fine-tuning, while Lifelong Few-Shot Customization tackles catastrophic forgetting in continual personalization (Song et al. 2024). These methods excel when a powerful foundation model exists, yet they inherit its biases and cannot generate outside the pre-trained support.

**Latent Space Manipulation.** A large body of work studies how to traverse or edit learned latent spaces to control semantics after training. Early observations on GANs reveal linear directions corresponding to gender or pose changes(Mehralian and Karasfi 2018). Deep Feature Interpolation interpolates between encoded features of two images to transfer attributes (Upchurch et al. 2017), and InterfaceGAN fits linear hyperplanes that dichotomise attributes in StyleGAN-2’s latent  $w$  space(Shen et al. 2020). More recently, transformer-based models have also been incorporated into latent space manipulation. For instance, Latent Space Editing in Transformer-Based Flow Matching (Hu et al. 2024) demonstrates how the flow-matching framework, traditionally used for generative tasks, can be extended to latent space editing in transformer models, enabling more precise control over the generated outputs. This work emphasizes the flexibility of latent space editing beyond the conventional GAN frameworks, offering a promising direction for models with more structured latent spaces. Additionally, the DepthFM (Gui et al. 2025) leverages flow matching in the latent space to generate high-quality depth maps from monocular images. This approach shows that flow matching can be used to manipulate the latent representations of images by focusing on the semantics of depth in the latent space.

## Method

Our goal is to develop a generative model that can produce high-fidelity samples from a target distribution using only few examples. This task is difficult because sparse data provides a weak training signal, which often leads to mode collapse or memorization. Our core insight is that this challenge can be addressed through the careful design of latent space geometry, combined with a principled iterative refinement process. We propose **Latent Iterative Refinement Flow (LIRF)**, which transforms the few-shot generation problem from learning a distribution over high-dimensional pixels to progressively densifying a well-structured latent manifold. Our key observation is that while pixel-space distributions are difficult to learn from sparse data, latent manifold can be systematically identified through geometric constraints and iterative correction mechanisms.

LIRF leverages a pre-trained autoencoder to map the data onto a manifold-preserving latent space. Within this space, we employ an iterative loop. A flow-matching model generates new candidate samples, which are then rigorously cor-

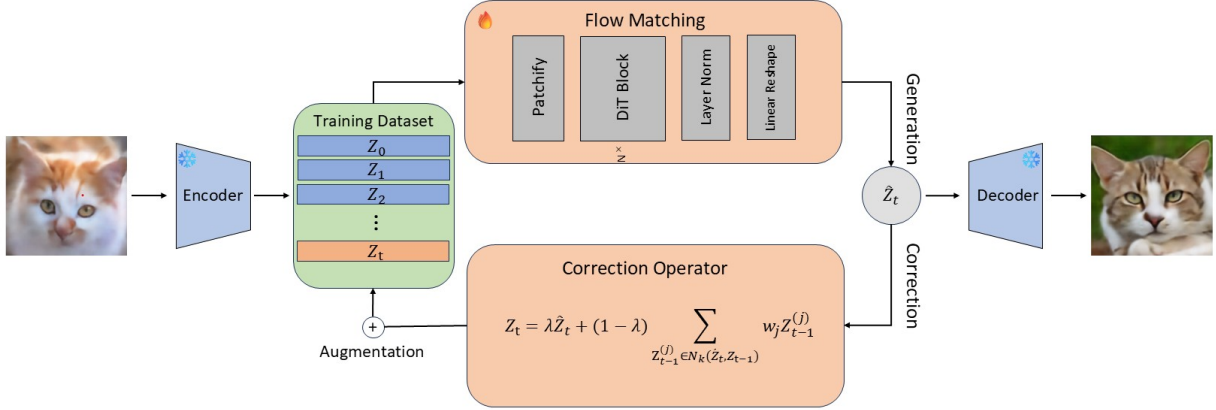


Figure 1: **Overview of training framework for LIRE.** The process begins by mapping the small training set to a latent space using a frozen autoencoder. This autoencoder is trained with a reconstruction loss and a novel manifold preservation loss to ensure the latent space retains the local geometric structure of the data. A flow-matching is then trained on these latent samples  $Z_0, \dots, Z_{t-1}$ . It generates new candidate samples  $\hat{Z}_t$ , which will be refined by a provably contractive correction operator based on whole training dataset. These corrected samples  $Z_t$  are then used to iteratively augment the training data. The final, high-fidelity outputs are produced by reconstructing the refined latent samples with the frozen decoder.

rected against the initial trusted data points before being used to augment the training set for the next iteration (See details in Algorithm 1). This process, illustrated in Figure 1, effectively bootstraps the limited initial data into a richer representation of the true data distribution. Crucially, this process is a theoretically guaranteed method with convergence proof to a high-quality generative model.

## I. Manifold-Preserving Latent Space

Standard generative models often operate in pixel space or in a latent space learned via simple reconstruction, where the geometric structure may not be meaningful. Our approach, in contrast, begins by establishing a latent space  $\mathcal{Z} \subset \mathbb{R}^d$  that explicitly preserves the local metric structure of the original data space  $\mathcal{X} \subset \mathbb{R}^D$ .

We achieve this using a fixed, pre-trained autoencoder, consisting of an encoder  $E : \mathcal{X} \rightarrow \mathcal{Z}$  and a decoder  $D : \mathcal{Z} \rightarrow \mathcal{X}$ . This autoencoder is trained with both a standard reconstruction loss (e.g., MSE) and a novel manifold-preservation loss  $L_{\text{manifold}}$ . This loss encourages the distances between neighboring points in the latent space to be proportional to their distances in the original pixel space. For a given point  $x_i$ , we define its local structure by its  $k$ -nearest neighbors. The loss  $L_{\text{manifold}}$  is formulated as:

$$\mathcal{L}_{\text{manifold}} = \frac{1}{Nk} \sum_{i=1}^N \sum_{j \in \mathcal{N}_k(x_i)} \left\| \sqrt{\frac{D}{d}} d(x_i, x_j) - d(z_i, z_j) \right\|_2^2. \quad (1)$$

where  $z_i = E(x_i)$ ,  $\mathcal{N}_k(\cdot)$  denotes the set of  $k$ -nearest neighbors with same label,  $d(\cdot, \cdot)$  is the distance between

two points. By minimizing  $L_{\text{manifold}}$ , we aim to achieve a latent space that is a locally bi-Lipschitz embedding of the original data manifold.

**Theorem 1 (Local Bi-Lipschitz Embedding)** *Let the data manifold  $\mathcal{M} \subset \mathbb{R}^D$  be a compact  $C^1$ -submanifold and the encoder  $E : \mathbb{R}^D \rightarrow \mathbb{R}^d$  be  $L_E$ -Lipschitz. If the autoencoder is trained to minimize  $\mathcal{L}_{\text{manifold}}$  such that for any  $x_i \in \mathcal{M}$  and its neighbors  $x_j \in \mathcal{N}_k(x_i)$ , the loss term approaches zero, then the mapping  $E|_{\mathcal{M}} : \mathcal{M} \rightarrow \mathcal{Z}$  is locally bi-Lipschitz. That is, for any  $x \in \mathcal{M}$ , there exists a neighborhood  $U \subset \mathcal{M}$  of  $x$  and constants  $0 < c_1 \leq c_2$  such that for all  $x_a, x_b \in U$ , the following holds:*

$$c_1 \|x_a - x_b\| \leq \|E(x_a) - E(x_b)\| \leq c_2 \|x_a - x_b\|$$

This theorem formally establishes that our latent space  $\mathcal{Z}$ , when equipped with the pullback metric, preserves the local geometric structure of  $\mathcal{M}$ . By pre-training the autoencoder with this objective, we establish a stable latent space  $\mathcal{Z}$ . In this space, the geometric proximity of points consistently corresponds to their semantic similarity, which is essential for the rest of our procedure. For the rest of the procedure, the autoencoder weights are frozen. The initial few-shot dataset  $S_0 = \{x_1, \dots, x_n\}$  is mapped to a set of latent "anchor" points  $Z_0 = E(S_0)$ , which we treat as initial trusted samples from the true latent data distribution  $q_{\text{data}}$ .

Given the manifold-preserving property of this latent space, we can now address a fundamental challenge in few-shot generation. Standard latent spaces, optimized purely for reconstruction, often distort the geometric relationships between samples. In contrast, our approach ensures that:

1. **Local neighborhoods are preserved:** Similar samples remain close in latent space.

2. **Interpolation is meaningful:** Linear combinations in  $\mathcal{Z}$  correspond to semantically coherent combinations in  $\mathcal{X}$ .
3. **Extrapolation is controlled:** The geometric structure guides exploration beyond the observed samples in a systematic way.

This latent space design is crucial for overcoming the limitations of traditional methods and significantly enhancing the model's ability to generate high-quality samples from sparse data.

## II. Manifold Densification

Given our geometrically-structured latent space, the few-shot generation problem is simplified to densifying the sparse data manifold represented by the anchor set  $Z_0$ . However, directly training a generative model on these few anchor points leads to poor sample quality due to the weak training signal. Our solution is an iterative refinement strategy that progressively expands the training set while maintaining fidelity to the original data distribution. The process alternates between three stages: generation, geometric correction, and data augmentation.

**Flow Matching in Latent Space** For generation, we turn to **Flow Matching (FM)**, a powerful class of generative models designed to regress vector fields based on fixed conditional probability paths(Liu, Gong, and Liu 2022; Lipman et al. 2023, 2024). FM has gained popularity for its ability to learn high-dimensional distributions stably and efficiently. We deliberately choose this method for two main reasons. First, training on a compressed latent space significantly reduces computational demands and is more data-efficient, which is crucial for handling high-resolution image data(Rombach et al. 2022). Second, unlike the notoriously unstable training dynamics of GANs and diffusion model in low-data regimes, Flow Matching offers a stable regression objective. This stability is essential for our iterative framework, which must reliably train on progressively augmented datasets.

The core principle of Flow Matching is to learn a time-dependent vector field  $v_\theta(z, t)$  that models the dynamics of a probability path  $p_t(z)$ . This path connects a simple prior distribution  $q_0 = q_{ref}$ (eg. a standard Gaussian  $\mathcal{N}(0, I)$ ), at  $t = 0$  to the target distribution  $q_1 = q_{data}$  at  $t = 1$ .

Flow Matching provides a highly efficient way to learn these dynamics. The general conditional flow matching objective (Tong et al. 2024) is to train the neural network  $v_\theta$  to match the conditional vector field  $u_t(z|z_1)$  by minimizing:

$$\mathcal{L}_{CFM}(\theta) = \mathbb{E}_{t, q_{data}(z_1), z \sim q_t(\cdot|z_1)} \|v_\theta(t, z) - u_t(z|z_1)\|_2^2 \quad (2)$$

Following common practice (Liu, Gong, and Liu 2022), we use a straight probability path  $z_t = tz_1 + (1-t)z_0$  conditioned on  $z_1 \sim q_{data}$  and  $q_0 \sim q_{ref}$ . At iteration  $t$ , we train  $v_{\theta_t}$  on the current dataset  $Z_{t-1}$  and generate candidate samples  $\tilde{Z}_t = \{\tilde{z}_1, \dots, \tilde{z}_m\}$ . However, due to data sparsity, these raw samples often exhibit poor quality or lie off the true manifold.

---

### Algorithm 1: Latent Iterative Refinement Flow (LIRF)

---

**Input:** dataset  $S_0 = \{x_i\}_{i=1}^n$ , pre-trained Encoder  $E$ , number of iterations  $T$ , generation batch size  $m$ , distance threshold  $\tau$ , neighbors  $k$ .  
**Initialize:** Anchor set  $Z_0 \leftarrow E(S_0)$ , Iterative training set  $Z_{\text{train}} \leftarrow Z_0$

- 1: Train initial flow model  $v_{\theta_0}$  on  $Z_{\text{train}}$ .
- 2: **for**  $t=0,1,\dots,T-1$  **do**
- 3:   // Step 1: Generate new samples
- 4:   Generate  $\tilde{Z}_t = \{\tilde{z}_j\}_{j=1}^m$  using the current flow model  $v_{\theta_t}$
- 5:   // Step 2: Correct generated samples
- 6:    $Z_{\text{corr}} \leftarrow \text{CorrectionOperator}(\tilde{Z}_t, Z_{t-1}, \tau, k)$ .{See Algorithm 2 for details.}
- 7:   // Step 3: Augment dataset and re-train
- 8:    $Z_t \leftarrow Z_{t-1} \cup Z_{\text{corr}}$
- 9:   Fine-tune  $v_{\theta_t}$  on  $Z_t$  to get  $v_{\theta_{t+1}}$
- 10: **end for**
- 11: **Output:** The final trained flow model  $v_{\theta_T}$

---

**Geometric Correction Mechanism** This stage is a core contribution of our work, designed to overcome the limitations of the small initial dataset  $Z_0$ . The key innovation is our correction operator  $\mathcal{C}$ , which leverages the geometric structure of the latent space to refine generated samples. This operator uses  $Z_{t-1}$  as a high-confidence representation of the data manifold and guides the newly generated samples  $\tilde{Z}_t$  toward a consistent geometry. This process consists of two steps: **Manifold Proximity Filtering** and **Geometric Refinement**.

First, we prune the generated set by filtering out any sample  $\tilde{z}$  that is too far from the known data manifold. We measure this by the sample's distance to the anchor set  $Z_{t-1}$ . A sample is kept only if it satisfies this condition:

$$\min_{z_i \in Z_{t-1}} d(\tilde{z}, z_i) \leq \tau \quad (3)$$

where  $\tau$  is a fixed distance threshold. This step ensures that we only consider augmenting our dataset with samples that are distributionally consistent with the original data. Let the set of filtered samples be  $\tilde{Z}_t$ .

Second, we refine each surviving sample  $\tilde{z} \in \tilde{Z}_t$  by pulling it towards its local neighborhood within the anchor set  $Z_{t-1}$ . The refined point  $\mathcal{C}(\tilde{z})$ , is calculated as a weighted average of its  $k$ -nearest neighbors in  $Z_{t-1}$ :

$$\mathcal{C}(\tilde{z}_t) = \lambda \tilde{z}_t + (1-\lambda) \sum_{Z_{t-1}^{(j)} \in \mathcal{N}_k(\tilde{z}_t, Z_{t-1})} w_j Z_{t-1}^{(j)}, \quad 0 < \lambda \leq 1 \quad (4)$$

where  $w_j = \frac{\exp(-\|\tilde{z}_t - Z_{t-1}^{(j)}\|_2)}{\sum_{Z_{t-1}^{(l)} \in \mathcal{N}_k(\tilde{z}_t, Z_{t-1})} \exp(-\|\tilde{z}_t - Z_{t-1}^{(l)}\|_2)}$ , an inverse distance weighting scheme, giving more influence to closer neighbors. The scalar  $\lambda$  acts as a weighting factor: a small  $\lambda$  emphasizes adherence to the anchor manifold, enhancing realism, while a  $\lambda$  approaching one allows greater deviation, thereby enriching diversity. The final set of corrected samples is  $Z_{\text{corr}} = \mathcal{C}(\tilde{Z}_t) = \{\mathcal{C}(\tilde{z}) \mid \tilde{z} \in \tilde{Z}_t\}$ . The entire routine

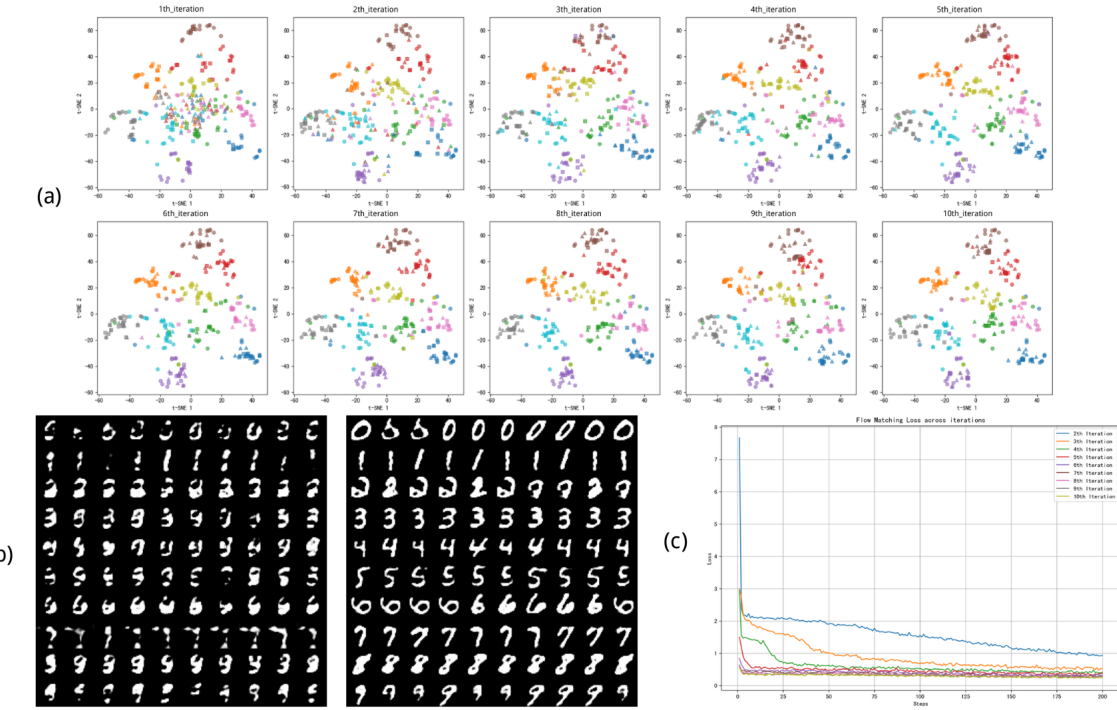


Figure 2: **Analysis of the framework’s mechanism on MNIST.** (a) Latent space visualization showing real samples (circles), candidate samples (triangles), and our corrected samples (squares). The color represents different labels of samples. Our correction pulls triangles towards circles, creating high-quality squares. In later iterations, triangles naturally fall closer to the circles. (b) Visual comparison of 1th iteration raw generated digit vs. its corrected version. (c) The overall Flow Matching loss decreases across iterations, confirming improved training stability and model fit to the augmented data distribution.

is distilled in Algorithm 2. Our operator projects generated samples back toward the reliable latent structure without stifling creative variation. In this way, the corrected samples  $\mathcal{C}(\tilde{Z})$  inherits both the fidelity of  $Z_{t-1}$  and the exploratory power of the generative model, striking a balance reminiscent of residual refinement in deep networks.

**Theorem 2 (Geometric Contraction of  $\mathcal{C}(\cdot)$ )** *Let  $\tilde{z}$  be a generated sample and  $Z_{\text{anchor}}$  be a set of anchor points. Let  $p(\tilde{z}) = \sum_{z_j \in \mathcal{N}_k(\tilde{z}, Z_{\text{anchor}})} w_j z_j$  be the local anchor point defined by the weighted average of the  $k$ -nearest neighbors of  $\tilde{z}$  in  $Z_{\text{anchor}}$ . The correction operator  $\mathcal{C}(\cdot)$  is a strict contraction mapping towards  $p(\tilde{z})$ , satisfying:*

$$\|\mathcal{C}(\tilde{z}) - \mathcal{C}(p(\tilde{z}))\| \leq \lambda \|\tilde{z} - p(\tilde{z})\|$$

where  $\lambda \in (0, 1)$  is the refinement weight.

This theorem formally establishes that our correction operator is a contractive mapping. Within the LIRF framework, this implies that corrected samples are consistently pulled towards the convex hull of the anchor set  $Z_{t-1}$ . The contractive property provides a key benefit: it allows us to balance fidelity to the original data distribution with the need for controlled exploration. This is made possible by our manifold-preserving latent space, which ensures that all refinements respect the data’s inherent geometry.

**Progressive Data Augmentation** The corrected samples  $Z_{\text{corr}} = \mathcal{C}(\tilde{Z}_t)$  are added to our training set:  $Z_t = Z_{t-1} \cup$

---

Algorithm 2: The Correction Operator ( $\mathcal{C}(\cdot)$ )

---

**Procedure** CorrectionOperator( $\tilde{Z}_t, Z_{t-1}, \tau, k$ )

**Input:** Generated samples  $\tilde{Z}_t$ , anchor set  $Z_{t-1}$ , distance threshold  $\tau$ , neighbors  $k$ .

```

1: // Stage 1: Filter out-of-distribution samples
2:  $\tilde{Z}_t \leftarrow \{\tilde{z} \in \tilde{Z} \mid \min_{z_i \in Z_{t-1}} d(\tilde{z}, z_i) \leq \tau\}$ .
3:  $Z_{\text{corr}} \leftarrow \emptyset$ 
4: // Stage 2: Refine surviving samples
5: for  $\tilde{z} \in \tilde{Z}_t$  do
6:   Find  $k$ -nearest neighbors  $\mathcal{N}_k(\tilde{z}, Z_{t-1})$  in the anchor
      set  $Z_{t-1}$ 
7:   Compute refined point  $\mathcal{C}(\tilde{z})$  using equation (4)
8:    $Z_{\text{corr}} \leftarrow Z_{\text{corr}} \cup \{\mathcal{C}(\tilde{z})\}$ 
9: end for
10: Output: The set of corrected samples  $Z_{\text{corr}}$ 

```

---

$Z_{\text{corr}}$ . This progressive densification of the data manifold ensures that each iteration adds high-quality samples that expand coverage while maintaining geometric consistency. The iterative process continues for  $T$  iterations, with each cycle improving both the Flow Matching model and the manifold approximation. The full procedure is detailed in Algorithm 1.

**Theorem 3 (Convergence of Iterative Process)** *Let the*

true latent manifold  $\mathcal{M}_{\mathcal{Z}} = E(\mathcal{M})$  be a compact  $d_m$ -dimensional submanifold of  $\mathcal{Z}$ . Under standard regularity assumptions, the sequence of augmented sets  $\{Z_t\}_{t=0}^T$  generated by the LIRF algorithm converges to the true manifold  $\mathcal{M}_{\mathcal{Z}}$ . The Hausdorff distance  $d_H(Z_t, \mathcal{M}_{\mathcal{Z}})$  is bounded as:

$$d_H(Z_t, \mathcal{M}_{\mathcal{Z}}) \leq C_1 \lambda^t + C_2 \tau (|Z_0| + m_{\text{eff}} \cdot t)^{-1/d_m}$$

where  $C_1, C_2$  are constants,  $\lambda \in (0, 1)$  is the contraction factor from the geometric correction,  $\tau$  is the filtering threshold,  $|Z_0|$  is the size of the initial anchor set, and  $m_{\text{eff}}$  is the effective number of samples added per iteration.

This theorem provides a formal guarantee for the long-term behavior of LIRF. It demonstrates that our iterative process effectively densifies the latent manifold and converges towards the true data distribution. The bound reveals an exponential decrease in the bias term (due to contraction) and a polynomial decrease in the covering error (due to augmentation), thereby establishing the predictable convergence of our method.

## Experiments

To validate the efficacy of our LIRF framework, we conducted a comprehensive set of experiments on multiple benchmark datasets. Our analysis demonstrates the model’s ability to generate high-quality samples from a limited number of training examples. We also analyze the contributions of our key components and position our performance against existing few-shot generative models.

**Experiment Setup.** For our autoencoder, we employ a convolutional architecture to learn a latent representation of the input data(Rombach et al. 2022). Our generative model is a Diffusion Transformer (DiT)(Peebles and Xie 2023) based Flow Matching network. For evaluation, we use the Fréchet Inception Distance (FID) as our primary metric to measure the perceptual quality and diversity of the generated samples. All experiments were conducted on NVIDIA A100 GPUs. We detail all hyperparameters, including the neighborhood size  $k$  and the distance threshold  $\tau$ , in the supplementary material.

We evaluate on three distinct datasets: MNIST (100 training images) to simulate a severe scarcity setting; CIFAR-10 (10% of the training data) as a standard benchmark for few-shot natural image generation; and AFHQ-Cat (5k images) to test performance on  $512 \times 512$  high-resolution images.

### I. Convergence Analysis of LIRF on MNIST

Our central hypothesis is that an iterative process of generation, correction, and augmentation can effectively learn a data distribution from a very small number of samples. To analyze this mechanism, we first conduct experiments on the simple MNIST dataset, using only 100 training images (10 per class).

We begin by visualizing the sample distributions in the latent space to dissect our framework’s behavior, as shown in Figure 2(a).The raw generated samples (triangles) from an early-stage model are often noisy and distant from the

real data manifold, which is represented by the ground-truth samples (circles). Our correction strategy effectively addresses this: the corrected samples (squares) are consistently pulled back into close proximity to the real data. This is a key observation: our correction mechanism successfully projects generated points onto the learned data manifold.

With these high-quality corrected samples used to augment the training data for the next cycle, the Flow Matching model itself improves. We observe that in later iterations, the raw generated samples (triangles) are produced progressively closer to the real data even before correction. This demonstrates the power of the iterative loop: a better generator produces better raw samples, which are then corrected to form an even higher-quality training set for the next iteration. As seen in the training dynamics Figure 2(c), the Flow Matching loss steadily decreases with each iteration, indicating a more stable and effective learning process. The qualitative results are equally stark, showing a clear transition from malformed digits to coherent ones as in supplement material.

This improved convergence translates directly to sample quality. The evolution of the Structural Similarity Index (SSIM), also shown in Table 1, reveals an increase with each iteration. The process culminates in a final SSIM that significantly surpasses a contemporary Quantum Diffusion Model(Chen et al. 2025) benchmark, as detailed in Table 1. This initial experiment, alongside the qualitative analysis, strongly supports our core hypothesis: iterative correction and data augmentation can successfully reconstruct a data distribution from very few samples.

Method	SSIM
EDM Diffusion Model(Karras et al. 2022)	0.1085
Quantum Diffusion Model(Chen et al. 2025)	0.1263
Our method(Iteration 1)	0.2051
Our method(Iteration 5)	0.2240
<b>Our method(Iteration 10)</b>	<b>0.2415</b>

Table 1: Iterative performance comparison on MNIST with 100 training samples. The table reports SSIM scores of diffusion-based baselines (top) and our method across iterations (bottom). Results demonstrate the progressive improvement of sample quality enabled by manifold-aware correction and iterative augmentation.

### II. Benchmark and Ablation Study on CIFAR-10

Having established the core mechanism of our framework on a simple dataset, we now assess its efficacy on the more complex CIFAR-10 (10% data) benchmark and dissect the source of its performance gains.

**Comparison with existing methods.** We first benchmark our method against several strong few-shot generation baselines. The results are presented in Table 2. Our framework achieves an FID of **30.29**, outperforming existing methods such as SNGAN, AdvAug, the Lottery Ticket Hypothesis and Patch Diffusion. This establishes our method as a competing solution for few-shot image generation.



Figure 3: **Samples from the AFHQ-Cat dataset.** Samples from the 10th iteration (bottom row) are substantially more detailed and realistic than those from the 1st iteration (top row), demonstrating the method’s scalability.

Method	FID
SNGAN(Miyato et al. 2018)	44.42
AdvAug(Cheng et al. 2020)	41.25
Lottery Ticket Hypothesis(Chen et al. 2021)	41.47
Lottery Ticket Hypothesis + AdvAug	33.32
Patch Diffusion(Wang et al. 2023)	40.11
Flow Matching (vanilla)	62.53
Ours (w/o $L_{\text{manifold}}$ )	41.23
<b>Our Method</b>	<b>30.29</b>

Table 2: Comprehensive comparison and ablation study on CIFAR-10 (10% Data). The table shows our method’s performance against existing baselines (top) and an ablation analysis of our framework’s components (bottom).

**Ablation Study.** Our main claim is that the synergy between our iterative loop and manifold-preserving latent space is essential. The ablation results in Table 2 provide clear evidence for this. First, we consider the Flow Matching (vanilla) baseline, which is equivalent to our framework without the iterative process. Its poor FID of 62.53 demonstrates that with severely limited data, a standard model cannot properly fit the true vector field. This causes the learned target distribution to shift, resulting in very poor image generation quality. Second, removing the manifold-preserving loss  $L_{\text{manifold}}$  results in a notable performance degradation. The absence of this regularization disrupts the geometric structure of the latent space, where Euclidean distance no longer reliably corresponds to perceptual similarity. This fundamentally undermines the efficacy of the nearest-neighbor-based correction mechanism. We observe that this leads to a degenerative cycle: ineffective corrections yield a low-quality augmented dataset for subsequent iterations, which in turn leads to a progressively deteriorating generative model, ultimately culminating in mode collapse.

### III. Scalability to High-Resolution Images

In additionIn Figure 3, we first investigate the impact of our iterative refinement framework on high-resolution image generation using the AFHQ-cat dataset. We observe that models from early iterations (e.g., iteration 1) produce images with noticeable artifacts and a lack of textural detail, a common outcome for generative models trained on limited

data. As the iterative process continues, the quality markedly improves. After 10 iterations, the framework generates images with substantially higher realism, sharper features, and improved global coherence. This provides strong visual evidence that our iterative correction and augmentation strategy successfully refines the learned data distribution.

### Conclusion

This paper introduces the Iterative Latent Refinement Flow (LIRF), a novel framework for few-shot generative modeling. Rather than directly modeling a complex pixel space distribution, LIRF constructs and progressively densifies the underlying data manifold within a geometrically structured latent space. This approach effectively mitigates overfitting and mode collapse in low-data regimes.

Our method is built on two key innovations: a manifold-preserving loss ( $L_{\text{manifold}}$ ) that ensures local structure preservation in the latent space, and an iterative refinement loop. The loop uses a flow-matching model to generate new samples, which are then refined by a novel, provably contractive correction operator. This iterative process enriches the training set and is theoretically guaranteed to converge.

Experimental results underscore LIRF’s effectiveness. On the CIFAR-10 benchmark, LIRF surpasses several existing methods, achieving competitive FID scores. A detailed analysis on MNIST further confirms the benefits of our iterative approach, showing consistent improvements in training loss and sample quality as the latent manifold becomes denser. Our ablation studies highlight that both the manifold-preserving loss and the iterative correction loop are indispensable, as removing either component leads to significant performance degradation. We also demonstrate our method’s scalability to high-resolution image synthesis on the AFHQ-Cat dataset.

LIRF represents a significant step toward data-efficient generative modeling without relying on massive pre-trained models. For future work, we plan to explore adaptive correction mechanisms and extend our iterative refinement paradigm to other modalities, such as video, audio, or 3D shapes. Overall, our approach offers a robust and principled solution for improving generative models in data-scarce scenarios.

## References

Chen, C.-S.; Hou, W. A.; Hu, H.-W.; and Cai, Z.-S. 2025. Quantum Generative Models for Image Generation: Insights from MNIST and MedMNIST. arXiv:2504.00034.

Chen, T.; Cheng, Y.; Gan, Z.; Liu, J.; and Wang, Z. 2021. Data-Efficient GAN Training Beyond (Just) Augmentations: A Lottery Ticket Perspective. In Ranzato, M.; Beygelzimer, A.; Dauphin, Y.; Liang, P.; and Vaughan, J. W., eds., *Advances in Neural Information Processing Systems*, volume 34, 20941–20955. Curran Associates, Inc.

Cheng, Y.; Jiang, L.; Macherey, W.; and Eisenstein, J. 2020. AdvAug: Robust Adversarial Augmentation for Neural Machine Translation. arXiv:2006.11834.

Dao, Q.; Phung, H.; Nguyen, B.; and Tran, A. 2023. Flow Matching in Latent Space. arXiv:2307.08698.

Dinh, L.; Krueger, D.; and Bengio, Y. 2014. NICE: Non-linear Independent Components Estimation. *arXiv preprint arXiv:1410.8516*.

Dinh, L.; Sohl-Dickstein, J.; and Bengio, S. 2016. Density estimation using Real NVP. *arXiv preprint arXiv:1605.08803*.

Duan, Y.; Niu, L.; Hong, Y.; and Zhang, L. 2024. Wedit-GAN: Few-Shot Image Generation via Latent Space Relocation. *Proceedings of the AAAI Conference on Artificial Intelligence*, 38(2): 1653–1661.

Gui, M.; Schusterbauer, J.; Prestel, U.; Ma, P.; Kotovenko, D.; Grebenkova, O.; Baumann, S. A.; Hu, V. T.; and Ommer, B. 2025. DepthFM: Fast Generative Monocular Depth Estimation with Flow Matching. *Proceedings of the AAAI Conference on Artificial Intelligence*, 39(3): 3203–3211.

Hu, V. T.; Zhang, W.; Tang, M.; Mettes, P.; Zhao, D.; and Snoek, C. 2024. Latent Space Editing in Transformer-Based Flow Matching. *Proceedings of the AAAI Conference on Artificial Intelligence*, 38(3): 2247–2255.

Karras, T.; Aittala, M.; Aila, T.; and Laine, S. 2022. Elucidating the Design Space of Diffusion-Based Generative Models. arXiv:2206.00364.

Lipman, Y.; Chen, R. T. Q.; Ben-Hamu, H.; Nickel, M.; and Le, M. 2023. Flow Matching for Generative Modeling. arXiv:2210.02747.

Lipman, Y.; Havasi, M.; Holderith, P.; Shaul, N.; Le, M.; Karrer, B.; Chen, R. T. Q.; Lopez-Paz, D.; Ben-Hamu, H.; and Gat, I. 2024. Flow Matching Guide and Code. arXiv:2412.06264.

Liu, X.; Gong, C.; and Liu, Q. 2022. Flow Straight and Fast: Learning to Generate and Transfer Data with Rectified Flow. arXiv:2209.03003.

Mehralian, M.; and Karasfi, B. 2018. RDCGAN: Unsupervised Representation Learning With Regularized Deep Convolutional Generative Adversarial Networks. In *2018 9th Conference on Artificial Intelligence and Robotics and 2nd Asia-Pacific International Symposium*, 31–38.

Miyato, T.; Kataoka, T.; Koyama, M.; and Yoshida, Y. 2018. Spectral Normalization for Generative Adversarial Networks. arXiv:1802.05957.

Peebles, W.; and Xie, S. 2023. Scalable Diffusion Models with Transformers. arXiv:2212.09748.

Rombach, R.; Blattmann, A.; Lorenz, D.; Esser, P.; and Ommer, B. 2022. High-Resolution Image Synthesis With Latent Diffusion Models. In *Proceedings of the IEEE/CVF Conference on Computer Vision and Pattern Recognition (CVPR)*, 10684–10695.

Ruiz, N.; Li, Y.; Jampani, V.; Pritch, Y.; Rubinstein, M.; and Aberman, K. 2023. DreamBooth: Fine Tuning Text-to-Image Diffusion Models for Subject-Driven Generation. arXiv:2208.12242.

Shen, Y.; Gu, J.; Tang, X.; and Zhou, B. 2020. Interpreting the Latent Space of GANs for Semantic Face Editing. In *Proceedings of the IEEE/CVF Conference on Computer Vision and Pattern Recognition (CVPR)*.

Song, N.; Yang, X.; Yang, Z.; and Lin, G. 2024. Towards Lifelong Few-Shot Customization of Text-to-Image Diffusion. arXiv:2411.05544.

Tong, A.; Fatras, K.; Malkin, N.; Huguet, G.; Zhang, Y.; Rector-Brooks, J.; Wolf, G.; and Bengio, Y. 2024. Improving and generalizing flow-based generative models with minibatch optimal transport. arXiv:2302.00482.

Upchurch, P.; Gardner, J.; Pleiss, G.; Pless, R.; Snavely, N.; Bala, K.; and Weinberger, K. 2017. Deep Feature Interpolation for Image Content Changes. arXiv:1611.05507.

Wang, Z.; Jiang, Y.; Zheng, H.; Wang, P.; He, P.; Wang, Z.; Chen, W.; and Zhou, M. 2023. Patch Diffusion: Faster and More Data-Efficient Training of Diffusion Models. arXiv:2304.12526.

Yang, R.; Jiang, B.; Chen, C.; Jin, R.; Wang, B.; and Li, S. 2024. Few-Shot Diffusion Models Escape the Curse of Dimensionality. In *The Thirty-eighth Annual Conference on Neural Information Processing Systems*.